Low-energy magnetic dipole radiation in open-shell nuclei

Schwengner, R.; Frauendorf, S.; Brown, B. A.;

Originally published:

March 2017

Physical Review Letters 118(2017), 092502

DOI: https://doi.org/10.1103/PhysRevLett.118.092502

Low-energy magnetic dipole radiation in open-shell nuclei

R. Schwengner,[1] S. Frauendorf,[2] and B. A. Brown[3]

[1]*Helmholtz-Zentrum Dresden-Rossendorf, 01328 Dresden, Germany*
[2]*Department of Physics, University of Notre Dame, Notre Dame, Indiana 46556, USA*
[3]*National Superconducting Cyclotron Laboratory and Department of Physics and Astronomy, Michigan State University, East Lansing, Michigan 48824, USA*

(Dated: March 24, 2017)

Low-energy $M1$ strength functions of ^{60,64,68}Fe are determined on the basis of large-scale shell-model calculations with the goal to study their development from the bottom to the middle of the neutron shell. We find that the zero-energy spike, which characterizes nuclei near closed shells, develops toward the middle of the shell into a bimodal structure composed of a weaker zero-energy spike and a scissorslike resonance around 3 MeV, where the summed strengths of the two structures change within only 8% around a value of 9.8 μ_N^2. The summed strength of the scissors region exceeds the total γ absorption strength from the ground state by a factor of about three, which explains the discrepancy between total strengths of the scissors resonance derived from (γ,γ') experiments and from experiments using light-ion induced reactions.

PACS numbers: 21.10.Pc, 21.60.Cs, 23.20.Lv, 27.50.+e

The excitation and deexcitation of the nucleus by electromagnetic radiation are fundamental processes in reactions of this many-body quantum system. At high excitation energy and high level density, statistical models are applied to describe reaction rates, which use γ-ray strength functions to describe the average transition strengths in a certain range of excitation energy. The experimental determination and the theoretical understanding of the properties of γ-ray strength functions has attracted increasing interest because of their importance for the accurate description of photonuclear reactions and the inverse radiative-capture reactions, which play a central role in in the synthesis of the elements in various stellar environments [1, 2].

Traditionally, the dipole strength function $f_1(E_\gamma)$, which is related to the experimental photoabsorption cross section $\sigma_\gamma = 3\ (\pi\hbar c)^2\ E_\gamma\ f_1(E_\gamma)$ of nuclei in the ground state, has been approximated with a Lorentz function characterizing the isovector electric dipole ($E1$) giant dipole resonance (GDR) [3–8]. In addition, the magnetic dipole ($M1$) absorption has been taken into account by two Lorentzians, which describe the scissors mode appearing in deformed nuclei around 3 MeV and the spin-flip mode appearing around 8 MeV [9], using parameters derived from systematics [5]. According to the so-called Brink-Axel hypothesis [3, 4] the strength function does not depend on the excitation energy and is identical for photoabsorption and photoemission following neutron capture or other compound-nucleus reactions.

In contrast to the decrease of the Lorentz curves toward $E_\gamma = 0$, an upbend of the dipole strength function below 2 MeV toward low γ-ray energy has been found in several nuclides in the mass range from $A \approx 50$ to 100, such as ^{56,57}Fe [10], ^{60}Ni [11], various Mo isotopes [12, 13], ^{105,106}Cd [14], and ^{151,153}Sm [15]. In addition to these results from light-ion induced reactions, the low-energy enhancement was also found in the β decay of ^{76}Ga [16]. All these experiments used the so-called Oslo method for extracting the γ-ray strength function. The existence of the low-energy enhancement was confirmed by using an alternative technique in Ref. [13]. The dominant dipole character of the low-energy strength was demonstrated in Ref. [17], and an indication for an $M1$ character of the low-energy strength was discussed for the case of ^{60}Ni [11]. The pronounced increase of the strength at low γ-ray energy may have a potentially large impact on neutron-capture reaction rates relevant for astrophysical processes [18].

In previous work [19], we have shown by means of shell-model calculations that the strengths of a large number of $M1$ transitions between excited nuclear states accumulate to an exponential spike in the γ-ray strength function, which peaks at zero transition energy, and that this low-energy magnetic dipole radiation (LEMAR) accounts for the low-energy enhancement of dipole strength observed in Mo isotopes around the neutron shell closure at $N = 50$. The large $B(M1)$ strength originates from transitions between initial and final states dominated by configurations with broken pairs of both protons and neutrons in high-j orbits, the spins of which recouple as $J_f = J_i, J_i \pm 1$. LEMAR was also found in shell-model calculations for ^{56,57}Fe [20] and ^{44,46}Ti [21]. The latter calculations also provided $E1$ strength functions, which decrease steadily toward $E_\gamma = 0$ in contrast to the upbend of the $M1$ strength. So far, all the shell-model calculations of the low-energy $M1$ strength have been carried out for nuclides around shell closures and all experiments except for that in Ref. [15] have identified LEMAR in nuclei near closed shells only. Therefore, the question arises of how the characteristics of low-energy $M1$ strength, in particular the LEMAR spike, develop in

nuclides with an increasing number of valence nucleons and increasing collectivity.

In this Letter, we analyze $B(M1)$ values obtained from large-scale shell-model calculations for the nuclides ^{60,64,68}Fe, which provide the first example of LEMAR in an isotope series extending to the middle of the shell between $N = 28$ and 50. We observe a weakening of the LEMAR spike and the development of a resonance around 3 MeV, which we interpret as the scissors mode based on excited states. The shift of $M1$ strength from the LEMAR spike to the scissors resonance approximately preserves the summed strength, which indicates a correlation between the two modes.

The calculations were carried out in the CA48PN model space with the CA48MH1 Hamiltonian [22] using the code NuShellX@MSU [23]. The model space included the $\pi(0f_{7/2}^{(6-t)}, 0f_{5/2}^{t}, 1p_{3/2}^{t}, 1p_{1/2}^{t})$ proton orbits with $t = 0$, 1, 2, and the $\nu(0f_{5/2}^{n5}, 1p_{3/2}^{p3}, 1p_{1/2}^{p1}, 0g_{9/2}^{g9})$ neutron orbits. We calculated the strengths of the quadrupole transitions from the yrast 2^+ state, $B(E2, 2_1^+ \rightarrow 0_1^+)$, using standard effective charges of $e_\pi = 1.5e$ and $e_\nu = 0.5e$. The values obtained for the occupation numbers $n5 = 2$ to 6 for all isotopes, $p3 = 0$ to 4 for ^{60}Fe and 2 to 4 for ^{64,68}Fe, $p1 = 0$ to 2 for all, and $g9 = 0$ to 2, 4 for ^{60,64}Fe and 2 to 6 for ^{68}Fe, respectively, are given in Table I. The further increase of $g9$ to 4, 6, 8 for ^{60,64,68}Fe, respectively, does not change the results considerably. The comparison with the experimental $B(E2)$ values in Table I shows that the calculations reproduce the quadrupole collectivity in the considered isotope series, in particular the considerable enhancement observed around $N = 40$ [24, 25]. The respective experimental ratios, $E(4_1^+)/E(2_1^+) = 2.57$, 2.48, 2.36, 2.45, 2.66, are reproduced by the calculated values, $E(4_1^+)/E(2_1^+) = 2.56$, 2.83, 2.68, 2.41, 2.43, respectively, and indicate the transitional character of the ground-state bands of all considered isotopes.

The calculations of $M1$ strengths included the lowest 40 states each with spins from $J_i, J_f = 0$ to 10. Effective g factors of $g_s^{\rm eff} = 0.9 g_s^{\rm free}$ were applied. The reduced transition strengths $B(M1)$ were calculated for all transitions from initial to final states with energies $E_f < E_i$ and spins $J_f = J_i, J_i \pm 1$. This resulted in more than 22000 $M1$ transitions for each parity, which were sorted into 0.1 MeV bins of their transition energy $E_\gamma = E_i - E_f$. The average $B(M1)$ value for one energy bin was obtained as the sum of all $B(M1)$ values divided by the number of transitions within this bin. The results of the $\overline{B}(M1)(E_\gamma)$ for $\pi = +$ and $\pi = -$ are shown in Figs. 1 and 2, respectively.

In ^{60}Fe LEMAR appears stronger for $\pi = -$ than for $\pi = +$ states. The difference is due to the $\nu 0g_{9/2}$ orbit that has to be occupied to generate negative-parity states, whereas its contribution to positive-parity states is smaller in this light isotope. This difference reaffirms our earlier observation [19] that the high-j orbits make

TABLE I: Experimental and calculated reduced $E2$ transition probabilities for the $2_1^+ \rightarrow 0_1^+$ transitions in ^{60,62,64,66,68}Fe.

	$E(2_1^+)$ (keV)		$B(E2, 2_1^+ \rightarrow 0_1^+)$ (W.u.)			β_2
	EXP[a]	CALC	EXP	GLOB[b]	CALC	CALC[c]
^{60}Fe$_{34}$	824	772	13.6(14)[d]	19.6	26.2	0.31
^{62}Fe$_{36}$	877	544	14.7(18)[e]	17.3	27.8	0.32
			13.6(17)[f]			
^{64}Fe$_{38}$	746	595	$30.9^{+13.8}_{-7.2}$[e]	19.1	26.8	0.32
			22.6(22)[f]			
^{66}Fe$_{40}$	574	568	21.0(21)[f]	23.4	27.8	0.32
^{68}Fe$_{42}$	522	616		24.2	25.4	0.31

[a] The values for ^{60,62,64,66,68}Fe were taken from Refs. [26–30], respectively.
[b] Value predicted from a global best fit according to Ref. [31].
[c] Quadrupole deformation deduced from the present calculated $B(E2)$ value according to the prescription given in Ref. [31].
[d] Value taken from Ref. [26].
[e] Value taken from Ref. [24].
[f] Value taken from Ref. [25].

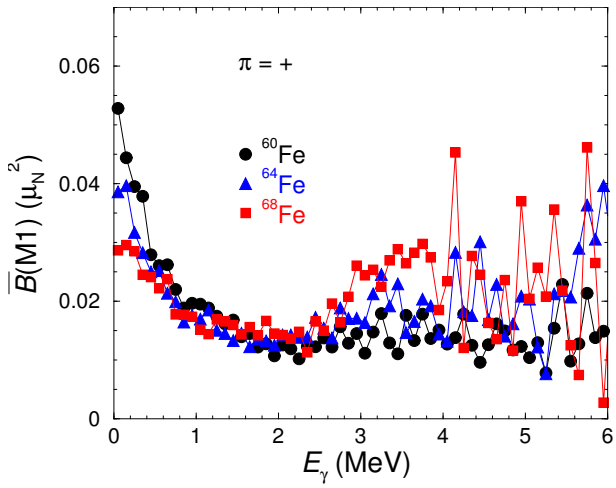

FIG. 1: (Color online) Average $B(M1)$ values in 100 keV bins of transition energy calculated for positive-parity states in ^{60}Fe (black circles), ^{64}Fe (blue triangles up), and ^{68}Fe (red squares).

the greatest contributions to the LEMAR spikes. The comparison of the $\overline{B}(M1)(E_\gamma)$ values of the various isotopes shows that the shape of the distributions changes when going from $N = 34$, four neutrons above the closed shell, to $N = 42$, the middle of the fpg shell. One observes a weakening of the LEMAR spike and the development of a bump in the range from about 2 to 5 MeV, which is most pronounced in ^{68}Fe. We interpret this bump as the scissors resonance (SR) built on excited states. The development of the bimodal LEMAR-SR structure can be attributed to the onset of stable quadrupole deformation above the yrast line when entering the open shell.

In Fig. 3, a map of $M1$ transitions between the cal-

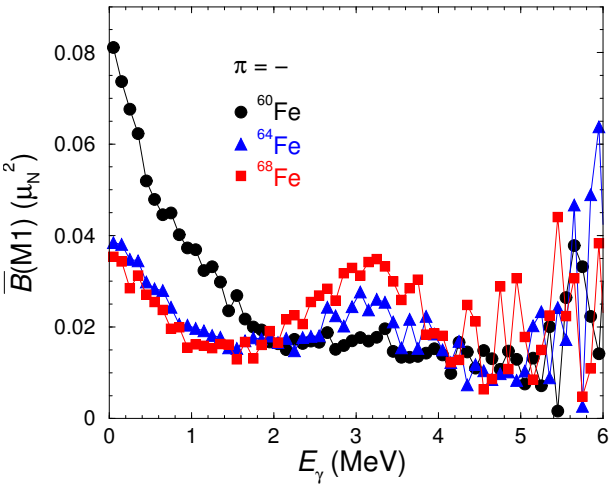

FIG. 2: (Color online) As Fig. 1, but for negative-parity states.

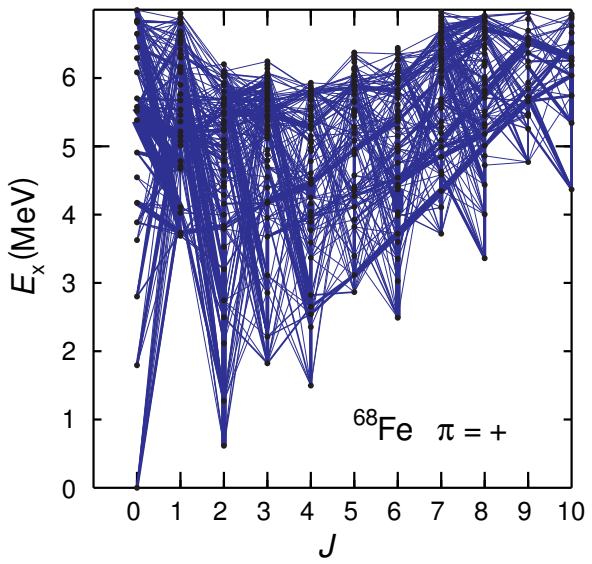

FIG. 3: (Color online) Transitions with $B(M1) > 0.1\mu_N^2$ (blue lines) between the calculated positive-parity states (black dots) in ^{68}Fe. The widths of the lines are proportional to the $B(M1)$ values.

culated states in ^{68}Fe is shown. There is a background of many transitions with $B(M1) < 0.1\mu_N^2$ (not shown for graphics reasons), which generate a large fraction of the LEMAR spike. On the visible background of chaotic transitions one recognizes bunches of transitions $J \to J \pm 1$ with transition energies of about 3 MeV [note the relative weight $(2J-1)/(2J+1)$], which are responsible for the scissors resonance. They are relatively weak in the analog figure for ^{60}Fe (not shown). These structures represent transitions between the different magnetic substates of the $g_{9/2}$ orbit, which are split by the presence of a deformed mean field. In the Nilsson model, the energy difference between 5/2 and 3/2 states is about 3 MeV at a deformation of $\varepsilon = 0.4$. The deformation is somewhat larger than the value in Table I, likely caused by the suppression of the of pair correlations with increasing excitation energy. In addition, one recognizes threads of transitions that form rotational sequences with $E_x \sim J(J+1)$. These structures correspond to shears bands (see e.g., Ref. [32]), observed near the yrast line of weakly deformed nuclei. The mechanism causing large $B(M1)$ values in these bands is reorientation of the high-j single-particle spins, as it is for LEMAR [19]. The difference is that the splitting of the $g_{9/2}$ states generates a degree of coherence in the reorientation reflected by the bandlike structures. These band structures are absent in ^{60}Fe.

Strength functions f_1 were deduced according to the prescription given in Ref. [19] using level densities from the present calculations and are shown in Fig. 4. The weakening of the LEMAR spike and the development of a resonance around 3 MeV with increasing neutron number are clearly seen in the $M1$ strength functions. The summed strengths deduced from the strength functions listed in Table II show that the total strength below 5 MeV varies by only 8% at most from an average of 9.80 μ_N^2. The slight increase with N is attributed to the progressive occupation of the $g_{9/2}$ shell for $N = 34$, 38, 42. For comparison, the standard $E1$ strength function with parameters taken from the RIPL data base [5] and $E2$ strength functions f_2 obtained from the present calculations as described in Ref. [33] are also shown in Fig. 4. The latter were multiplied with E_γ^2 to be directly comparable with the dipole strength functions f_1. The $E2$ strength $f_2 E_\gamma^2$ is more than one order of magnitude smaller and the $E1$ strength exceeds the $M1$ strength only at energies greater than 6 MeV. The bump at about 1.2 MeV for ^{68}Fe is caused by $E2, J \to J-2$ transitions, which organize into damped rotational bands of $E_x \approx J(J+1)/(2\mathcal{J})$ with a moment of inertia of $\mathcal{J} \approx 12$ MeV^{-1}. This is seen in a map analogous to the one in Fig. 3 and in individual plots of $\overline{B}(E2, J \to J-2)$ values, which show separate bumps at $E_\gamma \approx (2J-1)/\mathcal{J}$. The fact that the moment of inertia has twice the value of 5 MeV^{-1}, derived from the 2^+-state energy, indicates the presence of deformation and suppression of pair correlations with increasing excitation energy.

In the course of the present work, we learned of an experimental study of γ-ray strength functions of the well-deformed nuclides ^{151,153}Sm [15]. The strength functions deduced from these high-resolution experiments show for the first time a low-energy enhancement of dipole strength down to about $E_\gamma = 1$ MeV as well as a resonance around 3 MeV in one nuclide. The shapes of these strength functions in ^{151,153}Sm resemble the ones just discussed and can be taken as an experimental evidence of the bimodal structure in heavier nuclei. A striking feature of the scissors resonances observed in these

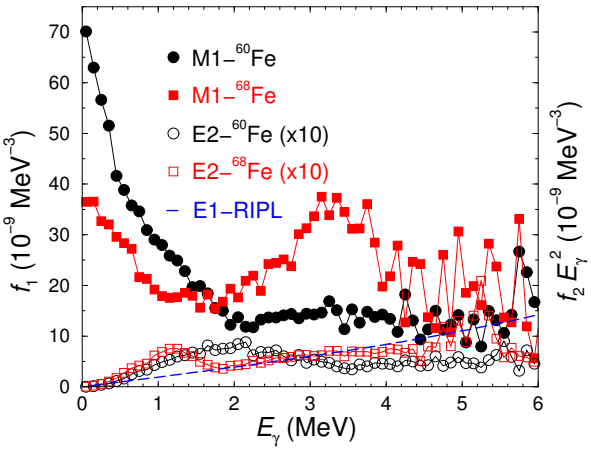

FIG. 4: (Color online) Strength functions deduced from the present calculations for ^{60}Fe and ^{68}Fe. Dipole strength functions f_1 deduced from average $B(M1)$ values are shown as filled black circles for ^{60}Fe and filled red squares for ^{68}Fe. The $E1$ strength function according to the RIPL data base [5] is shown as a blue dashed line. Quadrupole strength functions f_2 deduced from average $B(E2)$ values and multiplied with the transition energies are shown as open black circles and open red squares for ^{60}Fe and ^{68}Fe, respectively. Note that the $f_2 E_\gamma^2$ were multiplied by a factor of 10 to make them better visible.

TABLE II: Summed $B(M1)$ strengths deduced from the calculated strength functions for various ranges of transition energy, (LEMAR: $E_\gamma < 2$ MeV, Scissors: $2 \le E_\gamma \le 5$ MeV, Sum: $E_\gamma \le 5$ MeV), and summed strengths of all discrete transitions with $2 \le E_\gamma \le 5$ MeV from ground and first excited 0^+ states, respectively, to higher-lying 1^+ states.

	$B(M1)_{tot}$ (μ_N^2)			$\sum B(M1)(\mu_N^2)$	
	LEMAR	Scissors	Sum	$0_1^+ \to 1^+$	$0_2^+ \to 1^+$
^{60}Fe$_{34}$	5.67	3.52	9.19	0.66	1.98
^{64}Fe$_{38}$	4.46	5.13	9.59	1.65	2.59
^{68}Fe$_{42}$	3.98	6.63	10.61	1.74	3.45

experiments using the (p, d) reaction is that their total strength amounts to about 8 μ_N^2, which exceeds the typical strength found in (γ, γ') experiments by a factor of about two [9]. Similarly large values were found earlier for various actinides also studied via light-ion reactions [34].

In (γ, γ') experiments 1^+ states are excited from the ground state. The corresponding calculated $B(M1)$ values of the transitions in ^{68}Fe are shown in Fig. 5. The summed strengths of the individual transitions in the energy range from 2 to 5 MeV for the isotopes ^{60,64,68}Fe are listed in Table II. They are to be compared with the cumulative strengths of the f_1 functions in the same energy range, which contains the bump around 3 MeV seen in Fig. 4. Both quantities reflect the tendency of increasing strength in the scissors region when going to mid-

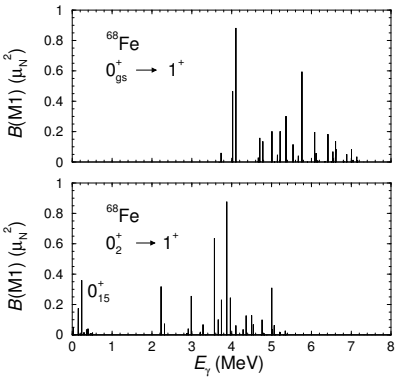

FIG. 5: Calculated $B(M1)$ values of transitions from the ground state to 1^+ states (upper panel) and from the second 0^+ state to 1^+ states (lower panel) in ^{68}Fe. In addition, transitions from the 15th 0^+ state to 1^+ states are shown in the lower panel below $E_\gamma = 1$ MeV.

shell nuclides. Furthermore, the cumulative strength of the transitions between excited states is larger than the cumulative absorption strength from the ground state. The ratio gives about three to be compared with a ratio of about two observed using light-ion reactions [15, 34].

The origin of the enhancement of the transition strength can be seen as an example in Fig. 5. There are more strong transitions with energies in the scissors region from the first excited 0_2^+ state to 1^+ states than from the ground state. As seen in Table II, their summed strengths from 2 to 5 MeV are about twice as large. In addition, transitions between the 0_{15}^+ state and 1^+ states are shown in Fig. 5. There are no transitions between these states in the energy range around 3 MeV because the highest calculated 1^+ state is located at 7.160 MeV and the 0_{15}^+ state lies at 6.648 MeV. One sees, however, that the $0_{15}^+ \to 1^+$ transitions also contribute to the LEMAR spike below about 1 MeV.

We attribute the larger summed strengths between excited states to a suppression of the pair correlations with increasing excitation energy, i.e. the thermal quenching of pairing. Pair correlations tend to couple the high-j or-

bits to zero spin, which obstructs the reorientation that generates the $M1$ radiation. The transition strengths between states of higher spins is expected to be additionally enhanced because of rotational quenching of pairing. These states contribute to the strength in the scissors region in the present calculations in correspondence to experiments with light ions.

For the first time the low-energy part of $M1$ strength function was investigated by means of large-scale shell-model calculations for a series of isotopes extending into the middle of an open shell. It was found that the zero-energy LEMAR spike, which characterizes nuclei near closed shells, develops into a bimodal structure composed of a weaker LEMAR spike and a scissorslike resonance around 3 MeV. In this process, the sum of the LEMAR strength and the strength in the scissors region varies by only 8% around a value of 9.8 μ_N^2. The summed strength of the strength function in the scissors region exceeds the total γ absorption strength in the ground state by a factor of about three, which is consistent with the typical strength found in (γ, γ') experiments and the strength derived from experiments using light-ion induced reactions. The present calculations show that this difference is generated by the greater number of transitions with large $M1$ strengths linking many excited states of various spins, which is attributed to a quenching of pair correlations.

S. F. acknowledges support by the DOE Grant DE-FG02-95ER4093, B. A. B. support by the NSF Grant PHY-1404442, and all authors acknowledge the importance of the ECT* workshop on "Statistical properties of nuclei", July 11 - 15, 2016, for advancing this research.

We thank the High-Performance Computing Center of Helmholtz-Zentrum Dresden-Rossendorf, the Center for Information Services and High-Performance Computing of Technische Universität Dresden, and the Center for Research Computing of the University of Notre Dame for their support.

[1] M. Arnould, S. Goriely, and K. Takahashi, Phys. Rep. **450**, 97 (2007).
[2] F. Käppeler, R. Gallino, S. Bisterzo, and W. Aoki, Rev. Mod. Phys. **83**, 157 (2011).
[3] D. M. Brink, Ph. D. thesis, Oxford University, 1955, unpublished.
[4] P. Axel, Phys. Rev. **126**, 671 (1962).
[5] R. Capote *et al.*, Nucl. Data Sheets **110**, 3107 (2009).
[6] A. Bohr and B. R. Mottelson, *Nuclear structure, vol. II*, (W. A. Benjamin, Inc., Reading, Massachusetts, 1975).
[7] J. M. Eisenberg and W. Greiner, *Nuclear theory, vol. I*, (North-Holland, Amsterdam, 1975).
[8] A. R. Junghans *et al.*, Phys. Lett. B **670**, 200 (2008).
[9] K. Heyde, P. von Neumann-Cosel, and A. Richter, Rev. Mod. Phys. **82**, 2365 (2010).
[10] A. Voinov *et al.*, Phys. Rev. Lett. **93**, 142504 (2004).
[11] A. Voinov *et al.*, Phys. Rev. C **81**, 024319 (2010).
[12] M. Guttormsen *et al.*, Phys. Rev. C **71**, 044307 (2005).
[13] M. Wiedeking *et al.*, Phys. Rev. Lett. **108**, 162503 (2012).
[14] A. C. Larsen *et al.*, Phys. Rev. C **87**, 014319 (2013).
[15] A. Simon *et al.*, Phys. Rev. C **93**, 034303 (2016).
[16] A. Spyrou *et al.*, Phys. Rev. Lett. **113**, 232502 (2014).
[17] A. C. Larsen *et al.*, Phys. Rev. Lett. **111**, 242504 (2013).
[18] A. C. Larsen and S. Goriely, Phys. Rev. C **82**, 014318 (2010).
[19] R. Schwengner, S. Frauendorf, and A. C. Larsen, Phys. Rev. Lett. **111**, 232504 (2013).
[20] B. Alex Brown and A. C. Larsen, Phys. Rev. Lett. **113**, 252502 (2014).
[21] K. Sieja, 5th International Conference on Collective Motion in Nuclei under Extreme Conditions (COMEX5), Sep. 14 - 18, 2015, Krakow, Poland; http://comex5.ifj.edu.pl/slides/sieja.pdf
[22] M. Hjorth-Jensen, T. T. S. Kuo, and E. Osnes, Phys. Rep. **261**, 125 (1995), and M. Hjorth-Jensen, private communication.
[23] B. A. Brown and W. D. M. Rae, Nucl. Data Sheets **120**, 115 (2014).
[24] J. Ljungvall *et al.*, Phys. Rev. C **81**, 061301(R) (2010).
[25] W. Rother *et al.*, Phys. Rev. Lett. **106**, 022502 (2011).
[26] E. Browne and J. K. Tuli, Nucl. Data Sheets **114**, 1849 (2013).
[27] A. L. Nichols, B. Singh, and J. K. Tuli, Nucl. Data Sheets **113**, 973 (2012)
[28] B. Singh, Nucl. Data Sheets **108**, 197 (2007).
[29] E. Browne and J. K. Tuli, Nuclear Data Sheets **111**, 1093 (2010).
[30] E. A. Mccutchan, Nucl. Data Sheets **113**, 1735 (2012).
[31] S. Raman, C. W. Nestor Jr., and P. Tikkanen, At. Data Nucl. Data Tables **78**, 1 (2001).
[32] S. Frauendorf, Rev. Mod. Phys. **73**, 463 (2001).
[33] R. Schwengner, Phys. Rev. C **90**, 064321 (2014).
[34] M. Guttormsen *et al.*, Phys. Rev. Lett. **109**, 162503 (2012).